6   **A New Tropical Savanna PFT, Variable Root Growth and Fire Improve Cerrado**

7   **Vegetation Dynamics Simulations in a Dynamic Global Vegetation Model**

9   Jéssica Schüler[1,2]*, Sarah Bereswill[2]*, Werner von Bloh[2],

10   Maik Billing[2], Boris Sakschewski[2], Luke Oberhagemann[2,3], Kirsten Thonicke[2] and

11   Mercedes M.C. Bustamante[1]

13   [1] Department of Ecology, University of Brasília, Campus Universitário Darcy Ribeiro,

14   70910-900, Brasília, Brazil

15   [2] Potsdam Institute for Climate Impact Research, Telegrafenberg A 31, 14473 Potsdam,

16   Germany

17   [3] Institute of Environmental Science and Geography, University of Potsdam, Karl-

18   Liebknecht Str. 24/25, Potsdam, Germany

20   *Correspondence to:* Jéssica Schüler (jehschuler@gmail.com)

21   **Abstract**

22   The Cerrado, South America's second largest biome, has been historically

23   underrepresented in Dynamic Global Vegetation Models (DGVMs). Therefore, this study

24   introduces a novel Plant Functional Type (PFT) tailored to the Cerrado biome into the

25   DGVM LPJmL-VR-SPITFIRE. The parametrization of the new PFT, called a Tropical

26   Broadleaved Savanna tree (TrBS), integrates key ecological traits of Cerrado trees,

27   including specific allometric relationships, wood density, specific leaf area (SLA), deep-

28   rooting strategies, and fire-adaptive characteristics. The inclusion of TrBS in LPJmL-VR-

29   SPITFIRE led to notable improvements in simulated vegetation distribution. TrBS became

30   dominant across Brazil's savanna regions, particularly in the Cerrado and Pantanal. The

31   model also better reproduced the above- and belowground biomass patterns, accurately

32   reflecting the "inverted forest" structure of the Cerrado, characterized by a substantial

33   investment in root systems. Moreover, the presence of TrBS improved the simulation of

34   fire dynamics, increasing estimates of burned area and yielding seasonal fire patterns more

35   consistent with observational data. Model validation confirmed the enhanced performance

36   of the model with the new PFT in capturing vegetation structure and fire regimes in Brazil.

37   Additionally, a global-scale test demonstrated reasonable alignment between the simulated

38   and observed global distribution of savannas. In summary, the integration of the TrBS PFT

39   marks a critical advancement for LPJmL-VR-SPITFIRE, offering a more robust

40   framework for investigating the interaction of above- with belowground ecological

41   processes, fire disturbance and the impacts of climate change across the Cerrado and other

42   tropical savanna ecosystems that together account for approximately 30 % of the primary

43   production of all terrestrial vegetation.

1. Introduction

46   The Cerrado, a biome of global importance and recognized as the world's most

47   biodiverse savanna, faces numerous challenges that threaten its rich biodiversity and the

48   vital ecosystem services it provides (Myers et al., 2000; Sano et al., 2019; Schüler and

49   Bustamante, 2022). The alarming deforestation rates, driven by agricultural expansion, and

50   the impacts of climate change, which are already exacerbating droughts and altering fire

51   dynamics, are the two main drivers of degradation, impacting water availability and

52   vegetation dynamics in this biome (Strassburg et al., 2017; Gomes, et al., 2020a; Rodrigues

53   et al., 2022).

54   Climate change impacts in Brazil are already evident. A study by INPE to the First

55   Biennial Transparency Report (MCTI, 2024) reveals an increase of approximately 20% in

56   the number of consecutive dry days in Brazil in recent decades, particularly in the North,

57   Northeast, and Central regions of the country. Similarly, Feron et al., (2024) demonstrated

58   an increase in the frequency of compound climate events involving heat, drought, and high

59   fire risk in key regions of South America, including the Amazon. A significant increase in

60   maximum and minimum temperatures was also observed in the Brazilian Cerrado between

61   1961 and 2019, along with a reduction in relative humidity (Hofmann et al., 2021).

62   In this context, vegetation modeling emerges as an essential tool for understanding and

63   predicting the Cerrado's responses to these pressures. Dynamic Global Vegetation Models

64   (DGVMs), such as the Lund-Potsdam-Jena managed Land model (LPJmL), aim to

65   simulate changes in vegetation, fire, water and carbon fluxes depending on climate and

66   land use (Cramer et al., 2001; Thonicke et al., 2010; Baudena et al., 2015; Moncrieff et al.,

67   2016; Schaphoff et al., 2018; Drüke et al., 2019; Martens et al., 2021). In order to reduce

68   complexity, common DGVMs classify vegetation into so-called Plant Functional Types

69   (PFTs), which are groups of plants that show similar responses to external drivers and

70   resemble their ecological function. PFTs are, in general, distinguished by their allometry,

71   growth form, phenology and photosynthetic strategy (Wullschleger et al., 2014).

72   Parameterization of PFTs should therefore capture the most important characteristics of

73   certain vegetation types while balancing complexity.

74   Specifically in savannas, vegetation is often characterized by small trees and shrubs that

75   grow deep roots and are well adapted to fire and drought, all of which distinguish them

76   from the trees in moist and seasonal tropical forests (Ratnam et al., 2011). However, many

77   DGVMs, including LPJmL, lack a dedicated savanna PFT, leading to significant

78   inconsistencies in model projections (Foley et al., 1998; Hughes, Valdes and Betts, 2006;

79   Clark et al., 2011; Neilson, R. P. 2015; Drüke; et al., 2019). This omission often results in

80   the underestimation of savanna vegetation extent and fire occurrences, while

81   overestimating above-ground biomass and the extent of tall tropical forest formations, as

82   demonstrated in simulations for South America (Cramer et al., 2001; Drüke et al., 2019),

83   or a depiction of savanna vegetation as tropical grasslands which do not encompass the

84   coexistence of grasses, shrubs and trees. DGVMs are, nevertheless, widely used to

85   simulate future transitions between the Amazon and the Cerrado biomes, often predicting

86   an abrupt shift from forest to grassland under climate change (Malhi et al., 2009; Swann

87   et al., 2015). However, this oversimplification neglects the intricate ecological gradient

88   that spans diverse vegetation types, from open forests to woody savannas with varying tree

89   cover densities.

90   This lack of precision in modeling has broader implications for understanding the

91   Cerrado's role in climate mitigation and adaptation, including nature restoration. For

92   example, restoring the entire 20 million hectares of the identified priority areas for

93   restoration in the Cerrado could remove up to 1.77 million tons of carbon from the

94   atmosphere (Schüler and Bustamante, 2022). Beyond carbon sequestration, savannas play

95   a crucial role in preserving water resources and biodiversity, acting as natural buffers

96   against climate change and enhancing ecosystem resilience (Oliver et al., 2015; Salazar et

97   al., 2016; Syktus and McAlpine 2016; Bustamante et al., 2019). With its highly seasonal

98   climate and diverse mosaic of grasslands, savannas, and forest formations, the Cerrado is

99   particularly significant for mitigating and adapting to climate change (Ribeiro and Walter

100 2008; Bustamante et al., 2019; Schüler and Bustamante 2022). Accurately representing

101 savanna-type vegetation in DGVMs will not only improve projections of the Cerrado's

102 vulnerability to climate change but also help identify high-risk areas and guide the

103 development of effective conservation, restoration, and management strategies. For

104 instance, improved models, acknowledging savanna-specific characteristics, could inform

105 studies investigating biome transitions and ecological tipping points, fire management

106 measures, support agricultural adaptation, and optimize water resource management,

107 ensuring the Cerrado's resilience in the face of environmental challenges.

108 We therefore introduce a new Cerrado specific PFT which we call "Tropical

109 Broadleaved Savanna tree" e (TrBS) that entails the biome's unique characteristics into a

110 state-of-the-art version of the LPJmL model (LPJmL-VR-SPITFIRE). LPJmL-VR-

111 SPITFIRE explicitly simulates variable tree rooting strategies (Sakschewski et al., 2021)

112 and employs the prossed-based fire model SPITFIRE (Thonicke et al., 2010;

113 Oberhagemann et al., 2025), while being based on the latest LPJmL version (LPJmL 5.7;

114 Wirth et al., 2024). In this study, we test our new approach by modeling the Potential

115 Natural Vegetation (PNV) distribution for the entire Brazil and validate our results against

116 observational datasets. This model improvement provides a robust basis for studies

117 exploring the impact of climate change on vegetation dynamics in the Cerrado region. This

118 model is expected to show significant improvements in biomass estimate, vegetation type

119 distributions, and fire dynamics in tropical regions.

2. Methods

2.1 Study region

Our study region encompasses all of the Brazilian territory, focusing on the distribution of its six biomes, with special attention to the Cerrado biome. Because of its central position, the Cerrado has ecotones with four of the other five Brazilian biomes: Amazon, Caatinga, Atlantic Forest and Pantanal (Fig. 1).

Brazil spans over 850 million hectares, extending from approximately 5ºN to 35ºS (IBGE, 2024). Due to its size, the country encompasses a wide range of climatic conditions, from subtropical and semi-arid regions to tropical wet environments (Table S1). The Cerrado, the second-largest vegetation formation in South America, covers about 23% of Brazil (~2 million km²), primarily in its central region (IBGE, 2024). Recognized as both a savanna and a global biodiversity hotspot, its seasonal precipitation regime is closely tied to the South American Monsoon System (Myers at al., 2000; Grimm, Vera and Mechoso, 2004). Its climate is predominantly classified as tropical savanna (Aw) according to the Köppen-Geiger classification system, characterized by a rainy season from October to April and a dry season from May to September (Peel et al., 2007; Oliveira et al., 2021). Annual rainfall ranges from 600 mm to 2,000 mm, with the highest averages near the Amazon border and the lowest near the Caatinga, and the mean annual temperature is 20.1°C (Sano et al., 2019).
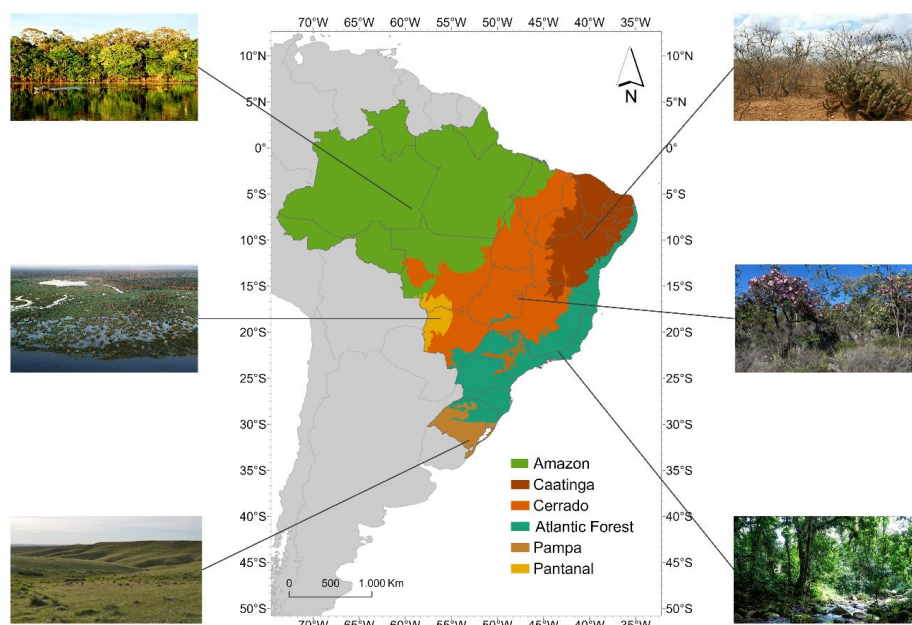
Fig. 1: Map representing the distribution of Brazilian biomes according to IBGE (2024) and photos showing their general appearances. Amazon photo by Andre Deak, Pantanal photo by Leandro de Almeida Luciano, Pampa photo by Ilsi Boldrini, Caatinga photo by Matheus Andrietta, Cerrado photo by Jéssica Schüler, and Atlantic Forest photo by Tânia Rego.

Historically, the biome is subject to periodic fires, especially in the grassland and savanna formations, highly influencing the evolution of its vegetation (Simon et al., 2009; Simon and Pennington 2012). Currently, fires predominantly occur at the end of the dry season, during September and October (Gomes et al., 2020; MapBiomas Fogo 2024). The vegetation in the Cerrado can be classified into three main vegetation formations: Forests, Savannas and Grasslands. Forest formations predominantly consist of trees forming a continuous canopy, typically found on deeper soils (Ribeiro and Walter 2008). Savanna formations are defined by the presence of both arboreal and herbaceous-shrub strata with

155 a canopy cover ranging from 5% to 70% and tree heights reaching 8 m on average (Ribeiro

156 and Walter 2008). Finally, grassland formations consist of shrubs and sub-shrubs

157 intermixed with herbaceous strata (Ribeiro and Walter 2008).

158

159 *2.2 Model description*

160   The LPJmL-VR-SPITFIRE model is a fire-enabled DGVM that integrates the latest

161 version of the DGVM LPJmL (LPJmL 5.7, Wirth et al., 2024) with the most recent

162 improvements of the SPITFIRE fire regime model (Thonicke et al., 2010; Oberhagemann

163 et al., 2025), together with the variable-roots (VR) developed by Sakschewski et al.,

164 (2021). This model framework enables the simulation of global vegetation dynamics,

165 including fire influence, fire disturbance (Schaphoff et al., 2018; Drüke et al., 2019).

166   LPJmL simulates the growth and productivity of both natural and managed vegetation,

167 considering water, carbon, and energy fluxes, and represents vegetation through PFTs

168 (Schaphoff et al., 2018). The model accounts for factors such as climate, soil, water, and

169 nutrient availability to simulate the distribution, biomass, and productivity of PFTs, and

170 has been validated against observational data on productivity, biomass, evapotranspiration

171 and PFT distribution on the global scale (Schaphoff et al., 2018). We briefly outline only

172 the most important features of the LPJmL-VR-SPITFIRE model version, while referring

173 to Schaphoff et al., (2018) for the general LPJmL model description.

174   *Variable roots:* In the original LPJmL model, a PFT-specific shape parameter β defines

175 tree rooting depth and fine root biomass distribution (Jackson et al., 1996). To better reflect

176 the diversity of rooting strategies of tropical trees, Sakschewski et al., (2021) introduced a

177 range of possible rooting strategies (shallow to deep rooted trees) per PFT, that can coexist

178 or outcompete each other. Unless constrained physically by soil depth or by available

179 resources, actual rooting depth is scaled with tree height via a logistic root growth function,

180   and new carbon pools (root sapwood and heartwood) represent the plant's investment in

181   growing coarse roots (Sakschewski et al., 2021). A long-term selection of the best suited

182   rooting strategies amongst each PFT is mediated by a modified tree establishment

183   approach, where the most successful rooting strategies can produce more saplings.

184   *Water-stress mortality*: Tree mortality in LPJmL depends on tree longevity, growth

185   efficiency and heat stress (Schaphoff et al., 2018). In this study, a new mortality component

186   reflecting mortality risk due to water stress has been included. This newly integrated water

187   stress mortality depends on tree phenology ($phen$) (Forkel et al., 2014, applied in

188   Schaphoff et al., 2018), leaf senescence due to water stress ($phen_{water}$) and PFT-specific

189   parameters representing water stress resistance (c_{res}) and sensitivity to drought (c_{sens}).

190   $$mort_{water} = c_{sens} \cdot phen \cdot (1 - phen_{water} - c_{res}) \qquad (1)$$

191   c_{sens} is a PFT-specific parameter that determines the overall sensitivity to drought stress.

192   *Phen* represents the actual phenological state of a tree, ranging from 0 (no leaf cover) to 1

193   (full leaf cover). This term accounts for the fact that trees with lower phenology (i.e., more

194   dormant trees) experience reduced water stress mortality. The expression $(1 - phen_{water})$

195   represents the intensity of leaf senescence due to low water availability (Forkel et al.,

196   2014), indicating that periods of reduced water availability lead to higher drought-induced

197   mortality. c_{res} defines a threshold below which drought-induced leaf senescence does not

198   significantly impact tree survival.

199   This model refinement allows for a more accurate representation of PFT-specific

200   sensitivity to water stress. Coupled with the variable rooting scheme, LPJmL-VR-

201   SPITFIRE allows trees to optimize the trade-off between carbon investment in deep roots

202   and aboveground growth, providing a survival advantage under drought conditions. The

203   PFT-specific parameters are found in Table 1.

204   *SPITFIRE* is a process-based fire model that simulates wildfire occurrence, spread, and

205   behavior, while considering fuel availability, fuel composition and weather conditions to

206   simulate ignitions, rate of spread and flame intensity (Thonicke et al., 2010). By coupling

207   SPITFIRE into LPJmL-VR (LPJmL-VR-SPITFIRE), SPITFIRE can simulate the

208   influence of fire on vegetation dynamics. Vegetation properties simulated by LPJmL-VR,

209   such as PFT composition and litter fuel moisture, determine the simulation of fire spread

210   and intensity which in turn influence post-fire vegetation conditions. SPITFIRE considers

211   both human-induced and natural ignitions, with the likelihood of these ignitions

212   developing into fires depending on the fire danger index of the modelled grid cell. Fires

213   then spread depending on factors such as dead and live fuel composition, wind speed, and

214   fuel moisture. We adopted the VPD (water vapor pressure deficit)-dependent calculation

215   of the fire danger index (Drüke et al., 2019; Gomes et al., 2020b) and the most recent

216   updates to the fire spread functions (Oberhagemann et al., 2025). Both the fire danger

217   index and rate of spread calculations include PFT-specific parameters that reflect different

218   vegetation related properties that affect ignition, fire duration and propagation. Fire-related

219   tree mortality is calculated considering PFT specific bark thickness (influencing cambial

220   damage) and scorch height (influencing crown mortality). Furthermore, with the recent

221   updates, SPITFIRE allows for multi-day fires and considers moisture of the live grass

222   share. SPITFIRE feeds back to the vegetation components by calculating fire effects on

223   the vegetation, such as fuel combustion and post-fire tree mortality (Drüke et al., 2019;

224   Oberhagemann et al., 2025).

225

226   ***2.3 Parameterization of a new Savanna tree PFT***

227   The Cerrado trees exhibit considerable morphological and physiological differences

228   compared to other tropical forest trees growing in closed canopy and wet environments.

229   Tree functional traits such as allometry, wood density, specific leaf area (SLA), rooting

230   depth, bark thickness, among others, contribute to a distinctive vegetation structure and

231   functioning, which are highly adapted to periodic drought and fire regimes. To incorporate

232   these characteristics into the LPJmL-VR-SPITFIRE model, we used a combination of

233   literature data and field observations to derive and calibrate the relevant parameters for the

234   new Tropical Broadleaved Savanna tree (TrBS) parametrization. A summary of all

235   parameters and data sources used is provided in Table 1 and 2, with detailed explanations

236   below.

237   *2.3.1 Allometry and growth form*

238   The tree allometry is defined through a diameter distribution that follows an asymptotic

239   pattern, where height increases at a slower rate as diameter grows larger, with most trees

240   remaining under 10 meters in height (Fig. S2A and C). A similar trend is observed in the

241   relationship between diameter and crown area: trees initially grow in diameter,

242   subsequently expanding their crown until crown growth reaches a plateau (Fig. S2B and

243   D). This observed growth pattern is implemented by allometric relationships using PFT-

244   specific allometric parameters within the LPJmL model (Schaphoff et al., 2018; Eqn. S1;

245   Eqn. S2). To ensure an accurate representation of TrBS's tree growth, we analyzed field

246   data to estimate maximum height, maximum crown area, and their relationship with stem

247   diameter (Table S2). Using these field measurements, we derived the allometric constant

248   values that best aligned with the observed data, by fitting the allometric equations to the

249   data (Fig. S2). Details about site location, data collected, and their references can be found

250   on Table S2.

251   Despite variations of wood density and SLA due to factors such as soil quality,

252   temperature, and water availability, trees in more arid environments typically develop

253   denser wood with lower SLA values (indicating thicker leaves), an adaptation to water

254   scarcity and mechanical stress (Scholz et al., 2008; Terra et al., 2018, Souza et al., 2024).

255   While we based our wood density value on literature (Souza et al., 2024), the SLA values

256   used in the development of TrBS PFT were estimated from field data collected from 71

257   individuals of 26 species (Table 1, Table S2).

258

259   Table 1: Allometry, drought mortality and rooting parameters used to define the new

260   Tropical Broadleaved Savanna Tree (TrBS) PFT, along with the corresponding values for

261   the Tropical Broadleaved Evergreen Tree (TrBE), and Tropical Broadleaved Raingreen

262   Tree (TrBR). References cited apply exclusively to TrBS PFT. Details about the field

263   survey data are available on Table S2. Additional information on TrBE and TrBR

264   parameters, as well as parameters not included in this table, can be found in Schaphoff et

265   al., (2018).

Parameter	Tropical Broadleaved Evergreen tree	Tropical Broadleaved Raingreen tree	Tropical Broadleaved Savanna tree	Reference
SLA ($mm^2 \cdot mg^{-1}$)	9.04	14.71	7.36	Field survey (Table S2)
Wood density ($g \cdot cm^{-3}$)	0.44	0.44	0.6	Souza et al., (2024)
Max. height (m)	100	100	10	Field survey (Table S2)
Max.crown area (m^2)	25	15	10	Field survey (Table S2)
Parameter in allometry function (*K-allom 1*)	100	100	153	Field survey (Table S2)

Parameter	Tropical Broadleaved Evergreen tree	Tropical Broadleaved Raingreen tree	Tropical Broadleaved Savanna tree	Reference
Parameter in allometry function (K-allom 2)	40	40	12	Field survey (Table S2)
Parameter in allometry function (K-allom 3)	0.67	0.67	0.52	Field survey (Table S2)
Maximum leaf-to-root-mass-ratio scaling parameter (lr_{max})	1	1	0.7	
Vertical root distribution parameter (β_{root})	[0.9418, 0.9851, 0.9925, 0.9950, 0.9963, 0.9971, 0.9976, 0.9981, 0.9986, 0.9993]			Sakschewski et al., (2021)
Shape parameter in logistic root growth function (k_{root})	0.02	0.02	0.07	Saboya and Borghetti (2012)

266

267   *2.3.2 Root growth and belowground carbon allocation*

268   Rooting depth is a crucial adaptation for the Cerrado species, enabling access to deep

269   water reserves during prolonged dry periods (Oliveira et al., 2005; Tumber-Dávila et al.,

270   2022). Due to its high investment in belowground structures, the Cerrado is often referred

271   to as an 'upside-down forest,' storing approximately five times more carbon below-ground

272   (in roots and as soil carbon) than above-ground (Terra et al., 2023). While deep roots are

273   a well-documented feature of the Cerrado plants, rooting strategies vary widely among

274   species. To try to reflect this diversity in rooting strategies in LPJmL-VR-SPITFIRE we

275   allowed for 10 different root distributions (β_{root} parameter) per PFT. We chose the same

276   range of β_{root} values for TrBS PFT as for the other PFTs, to allow a spectrum of shallow,

277   intermediate and deep rooting strategies to compete. From β_{root} the depth where 95% of

278   root biomass are found (D95) can be calculated (see Sakschewski et al., 2021). Studies

279   show that the Cerrado tree seedlings invest more in root growth compared to shoot growth

280   as a strategy to access water deeper in soil during the dry season (Hoffmann, Orthen and

281   Franco 2004; Saboya and Borghetti 2012). We reflect this by modifying the shape

282   parameter of the logistic root growth function (k_{root}, Table 1), to allow TrBS to reach

283   deeper rooting depths already earlier in their lifecycle (Fig. 2), enhancing the underground

284   competitiveness of these savanna trees. In LPJmL-VR-SPITFIRE, carbon allocation to

285   coarse woody roots is represented by separate root sapwood and heartwood carbon pools,

286   introduced in addition to the fine root carbon pool (Sakschewski et al., 2021). Due to the

287   necessary balance between root and stem sapwood investment (Pipe Model approach;

288   Shinosaki et al., 1964), and the relationship between tree height and rooting depth, deep

289   root growth for TrBS saplings represents a trade-off between above- and belowground

290   growth.

291   The ratio between the leaf and the fine root biomass in the model depends on the

292   model internally calculated water stress index (ω), where more root biomass is built

293   under water stress, and is constrained by the lr_{max} (maximum leaf-to-root-mass-ratio)

294   scaling parameter (Table 1; Schaphoff et al., 2018). We set lr_{max} to 0.7 to allow TrBS to

295   invest relatively more into root biomass than the other tropical tree PFTs, where lr_{max} was

296   set to 1 (Schaphoff et al., 2018).

297

298
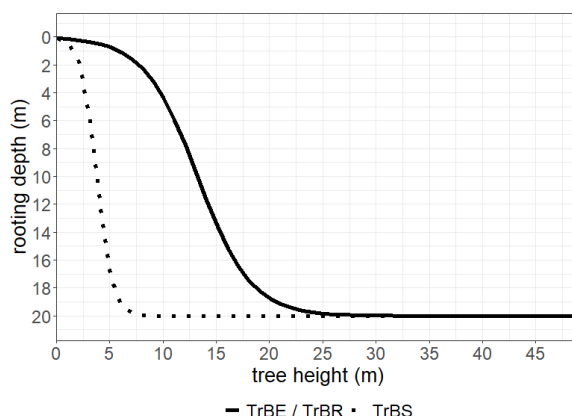
Fig. 2: Logistic growth function scaling rooting depth to tree height, shown for a soil depth

300   of 20m for the different PFTs (TrBE = tropical broadleaved evergreen, TrBR = tropical

301   broadleaved raingreen, TrBS = Tropical Broadleaved Savanna).

302

303   *2.3.2 Phenology*

304   The Cerrado exhibits pronounced precipitation seasonality, which shapes the

305   phenology of its vegetation. Deciduous and semi-deciduous species display leaf dynamics

306   in which leaves shed during the dry season, peaking in July, and sprout during the

307   transition to the rainy season in September (de Camargo et al., 2018). Despite the

308   dominance of deciduous and semi-deciduous species (74%), the community rarely

309   experiences complete defoliation, retaining at least half of its foliage in most years (de

310   Camargo et al., 2018). This seasonal pattern is also evident in the Leaf Area Index (LAI)

311   of trees. LAI values drop from around 1 in the rainy season to approximately 0.6 on the

312   peak of the dry season (Hoffmann et al., 2005).

313   The degree of foliation in LPJmL-VR-SPITFIRE is given by the phenology status,

314   which is updated daily (ranging from 0 = no leaves to 1 = full leaf cover) and derived by

315   multiplication of four limiting functions, namely a water-limiting (f_{water}), light-limiting

316   (f_{light}), cold-limiting (f_{cold}) and heat-limiting (f_{heat}) function (Schaphoff et al., 2018;

317   Forkel et al., 2014). The shape parameters of f_{water} were chosen to reflect a behaviour

318   intermediate between the evergreen and the raingreen PFT (Fig. S3), and thereby reflects

319   the general phenological behaviour of the Cerrado community as explained above; f_{heat},

320   f_{cold} and f_{light} were set to the same values as for TrBE.

321   *2.3.4 Fire dynamic and vegetation adaptation*

322   Approximately 6 million hectares burned in the Cerrado in 2023 (MapBiomas Fogo

323   2024), with 98% of these fires attributed to human activity (Schumacher et al., 2022). At

324   local and landscape scales, fire dynamics are influenced by factors such as fuel availability,

325   ignition sources, topography, and climatic conditions (Gomes, Miranda, and Bustamante

326   2018). In the Cerrado, fire behavior is closely tied to seasonal cycles and one key factor

327   determining its behavior is the vapor pressure deficit (VPD) (Gomes, et al., 2020b; Oliveira

328   et al., 2021). VPD is the measure of the difference between the vapour pressure of the

329   moisture present in the air and the maximum vapour pressure the air can hold, being

330   influenced by temperature and relative humidity. In the Cerrado, the VPD varies

331   seasonally, with average values around 0.3 to 0.7 kPa in the rainy season and 1.4 to 2.0

332   kPa in the dry season (Cattelan et al., 2024). Higher VPD dehydrates plant biomass,

333   especially from grasses, making it more flammable and susceptible to fire (Gomes, et al.,

334   2020b). The VPD affects the rate of spread and intensity of the fire, with higher VPD

335   resulting in faster and more intense fires in a given fuel bed (Gomes et al., 2020b; Oliveira

336   et al., 2021). In LPJmL-VR-SPITFIRE, the fire danger index depends on VPD and is

337   scaled via a PFT-specific factor **α**VPD, where higher values of **α**VPD increase fire danger.

338   We calibrated **α**VPD to achieve good agreement between observed and modelled burnt

339   area. A higher **α**VPD for TrBS than for TrBE and TrBR was chosen, because the fuel

340   produced by the Cerrado trees burns more readily, compared to the fuel dropped by trees

341   in the moist forests (dos Santos et al., 2018).

342   Because of its fire-prone environment, the Cerrado trees exhibit several adaptations that

343   enable them to survive fire damage. These include belowground organs that promote

344   resprouting after fire, thick bark that insulates and protects internal tissues, robust terminal

345   branches, leaves concentrated at branch tips, and persistent stipules that safeguard apical

346   buds, all minimize fire damage (Simon et al., 2009; Simon and Pennington 2012). Fire-

347   induced tree mortality in LPJmL-VR-SPITFIRE results from combined effects of cambial

348   and crown damage (Oberhagemann et al., 2025). PFT-specific parameters for bark

349   thickness were chosen to fit the relationship between stem diameter and bark thickness

350   shown in Hofmann et al., (2009) (Fig. S3; Table 2). Scorch height, the highest point at

351   which flames reach and affect the vegetation, is calculated from fire intensity and a PFT

352   specific scaling factor (F; see Eqn. S5), which also depends on tree crown length relative

353   to its height (Thonicke et al., 2010; Oberhagemann et al., 2025). The Cerrado trees have

354   relatively long crowns compared to their total height, with a ratio of 0.53 (Table 2). While

355   this exposes them to crown scorch, the above-mentioned adaptations result in an overall

356   lower mortality risk from crown scorch, and we therefore adjusted the parameter F

357   accordingly (Table 2).

358

359

360

361   Table 2: Fire parameters used to define the new Tropical Broadleaved Savanna Tree

362   (TrBS) PFT, along with the corresponding values for the Tropical Broadleaved Evergreen

363   Tree (TrBE) and Tropical Broadleaved Raingreen Tree (TrBR) PFTs. References cited

364   apply exclusively to TrBS PFT. SPITFIRE parameters for TrBE and TrBR are taken from

365   (1) Thonicke et al., (2010), and (2) Drüke et al., (2019).

Parameter	Tropical Broadleaved Evergreen tree	Tropical Broadleaved Raingreen tree	Tropical Broadleaved Savanna tree	Reference
Leaf Longevity (*years*)	1.6	0.5	1	Cianciaruso et al., (2013); Souza, J. P. (2012)
Sensitivity to drought (c_{sens})	100	100	10	
Water stress resistance (c_{res})	0.1	0.1	0.1	
Water limitation factor ($wscal_{min}$)	0	0.35	0	
αVPD	6	6	10	
Crown length parameter	0.3334 [1]	0.10 [1]	0.53	Field survey (Table S2)
Scorch height parameter (*F*)	0.193 [2]	0.0799 [2]	0.13	
Bark thickness par1/par2	0.0301/0.0281 [1]	0.1085/0.212 [1]	0.135/0.2820	Hoffmann et al., (2009)

366

367   ***2.4 Simulation protocol***

368   To evaluate the performance of the newly implemented TrBS PFT, two simulation runs

369   were conducted: one including TrBS PFT (hereafter 'Savanna' simulation) and the other

370   experiment excluding it (hereafter 'No Savanna' simulation). Both simulations covered

371   the period from 1901 to 2019, with a 5000-year spin-up phase, and utilized identical

372   environmental input data in a 0.5º horizontal resolution.

373   The model spin-up was simulated from bare ground using climate input from 1901-

374   1930 (with pre-industrial pCO_2 = 276.59 ppm), which was repeated for 5000 years, to

375   allow carbon pools to reach equilibrium with climate. The transient simulation then ran

376   from 1901 to 2019. For model validation, we analyzed the last 30 years of the transient

377   run. Because we aim to evaluate the establishment and general characteristics of the new

378   TrBS PFT, all simulations were conducted for potential natural vegetation (PNV) only,

379   with no simulation of human land use to focus on geographical distribution of vegetation

380   and fire. While LPJmL-VR-SPITFIRE features the latest model updates regarding the

381   nitrogen cycle (Bloh et al., 2018) and biological nitrogen fixation (Wirth et al., 2024), we

382   switched the nitrogen limitation off as it was beyond the scope for this study.

383   The LPJmL-VR-SPITFIRE model uses daily climate input, including air temperature,

384   precipitation, wind speed, humidity, and long- and shortwave radiation. These datasets

385   were sourced from ISIMIP3a (https://data.isimip.org/10.48364/ISIMIP.664235.2), which

386   combines GSWP3 data (1901–1978) and W5E5 data (1979–2019). Atmospheric CO_2

387   concentration data were derived from the TRENDY project (Friedlingstein et al., 2023) .

388   Soil texture data were obtained from the Harmonized World Soil Database

389   (Nachtergaele et al., 2009). Soil depth in LPJmL-VR-SPITFIRE was defined using the

390   lower water table depth values provided by the SOIL-WATERGRIDS dataset (Guglielmo

391   et al., 2021).

392   Ignition sources for the SPITFIRE model are based on population density (Klein

393   Goldewijk et al., 2011) for human ignitions, and lightning occurrence data from the

394   OTL/LIS dataset (Christian et al., 2003) for natural ignitions.

395

396 ***2.5 Model validation***

397   For each of our simulation outputs, we selected appropriate Brazilian or global datasets

398 to validate the modeled results from LPJmL-VR-SPITFIRE. All spatial analysis and

399 comparisons between the validation data and model outputs were conducted in R, utilizing

400 the ncdf4, terra, raster and sf packages. The analysis focused on the mean values of the last

401 30 years of the simulations (1990-2019). Details of each validation dataset are provided

402 below.

403 *2.5.1 Vegetation distribution*

404   To validate the modeled distribution of the vegetation in Brazil, represented by the

405 foliar projected coverage (FPC) of each PFT, we used Brazil's original vegetation

406 distribution by IBGE (2017). The original IBGE map was a very detailed Shapefile, with

407 specific variation of each major vegetation group, that would have complicated the

408 comparison with the FPC and limited number of PFTs. For this reason, we aggregated the

409 vegetation classes into 13 vegetation types following the attribute table of IBGE's product

410 (Fig. 4). After that, we converted the Shapefile into a raster file using the function rasterize

411 from the terra package in R.

412   To evaluate the distribution of the new TrBS PFT, as well as the other tropical PFTs,

413 we overlaid the FPC output with the corresponding classification from IBGE. For this

414 comparison, we selected only grid cells where the respective FPC $\geq$ 0.3 and matched the

415 class in the IBGE dataset, generating a map that identifies under-, over-, and correctly

416 simulated PFT coverage.

417   *2.5.2 Above- and belowground Biomass, evapotranspiration and productivity*

418   The above- and belowground biomass (AGB and BGB) validation maps were produced

419   by the team from the Fourth National Communication to the United Nations Convention

420   of Climate Change, here referred to as QCN (MCTI 2020). These maps were produced

421   considering the distribution of Brazil's original vegetation (IBGE 2017) and estimating

422   AGB and BGB using specific equations and field data that best fit each vegetation type.

423   From these maps we derived a BGB:AGB ratio map to validate the structural

424   characteristics of TrBS PFT. For better comparison, we calculated the Spearman

425   Correlation between the two modeled scenarios of BGB:AGB and the QCN validation

426   using the stats package from R software.

427   For evapotranspiration (ET) and gross primary productivity (GPP), the mean annual

428   distribution of the last 30 simulation years (1990-2019) were compared to reference

429   datasets (GPP: Carvalhais et al., 2014; ET: ERA-Interim-Land, Balsamo et al., 2015) and

430   evaluated via the Normalized Mean Squared Error (NMSE) and Pearson correlation (as

431   described in Sakschewski et al., 2021).

432   *2.5.3 Burned Area*

433   The Burned Area validation map was produced using the annual burned coverage

434   product from MapBiomas Fogo 3.0 (2023) database. This product gives a 30 m resolution

435   presence-absence map of areas in which fire occurred for a time series from 1985 to 2023.

436   The burned area was calculated from the burned coverage for a 0.5° grid, covering all the

437   Brazilian territory, for each year from 1990 to 2018. Then, from resulting annual burned

438   area maps, we calculated the mean burned area for all selected time series. All calculations

439   and map generation from the MapBiomas dataset were performed using the Google Earth

440   Engine platform.

441   For the spatial distribution of annual burned area, we created a map of the human land-

442   use fraction based on MapBiomas 9.0 land-use data (MapBiomas, 2023), using the mean

443   value from 1990 to 2019 (Fig. S5). Since our simulation considers only potential natural

444   vegetation (PNV), we weighed the burned area, in both the validation data and model

445   output, to account for fire occurrences in human-managed land.

446   The validation of the monthly burned area for the Cerrado biome was conducted using

447   the MapBiomas Fogo 3.0 dataset (2023). The burned area validation was also weighed by

448   the natural land-cover of the corresponding year. This dataset was used to assess the

449   accuracy of the simulated seasonal burned area patterns in the Cerrado. The comparison

450   between the simulated scenarios and the MapBiomas data was evaluated using Normalized

451   Mean Squared Error (NMSE), Willmott's index, R^2, and p-value statistics from the

452   respective R packages kerntools, hydroGOF and stats (Drüke et al., 2019).

453   For carbon emission by fire (FireC), our validation is based on the Global Fire

454   Emissions Database (GFED4), which derives its fireC emission maps using its own burned

455   area data (van der Werf et al., 2017). GFED4 combines satellite observations of burned

456   area with biogeochemical modeling to estimate emissions of CO_2, CO, CH_4, and other

457   trace gases. Given the strong link between burned area and fire emissions, we apply the

458   same land-use fraction weighting approach as for burned area to ensure consistency in our

459   analysis.

3. Results

3.1 Vegetation distribution

460
461
462   The inclusion of TrBS PFT has significantly altered the distribution and abundance

463   of key vegetation types across Brazil, particularly the Tropical C_4 grasses and TrBE

464   PFTs. In simulations without TrBS, C_4 grass dominates across northeastern and central

465   Brazil, occupying the whole Caatinga biome, most of the Cerrado and northern Atlantic

466   Forest (Fig. 3).

467   TrBS establishes itself predominantly in the Cerrado and Pantanal biomes, aligning

468   with regions classified as savanna vegetation by IBGE (Figs. 3 and 4). Pockets of TrBS

469   also appear in northern portions of the Amazon biome, where patches of savanna-like

470   vegetation can occur, and Atlantic Forest regions where seasonal forest is present (Fig.

471   3 and 4). The presence of TrBS results in a contraction of C_4 grass, which retreats mostly

472   to the Caatinga biome, where they almost entirely dominate due to Caatinga's dry

473   environment, while grass and savanna vegetation coexist in Pantanal, northern and

474   eastern Cerrado (Fig. 3).

475

476
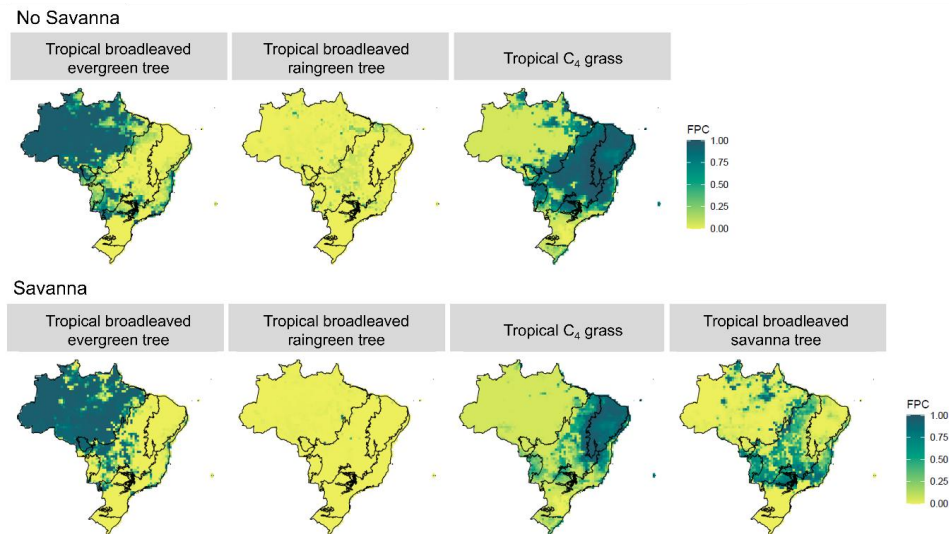
477 Fig. 3: Foliar Projected Cover (FPC) of the Plant Functional Types (PFT) for Tropical

478 Broadleaved Evergreen Tree, Tropical Broadleaved Raingreen Tree, Tropical C_4 Grass

479 and Tropical Broadleaved Savanna Tree in Brazil under two model configurations: 'No

480 Savanna' and 'Savanna'.

481

482
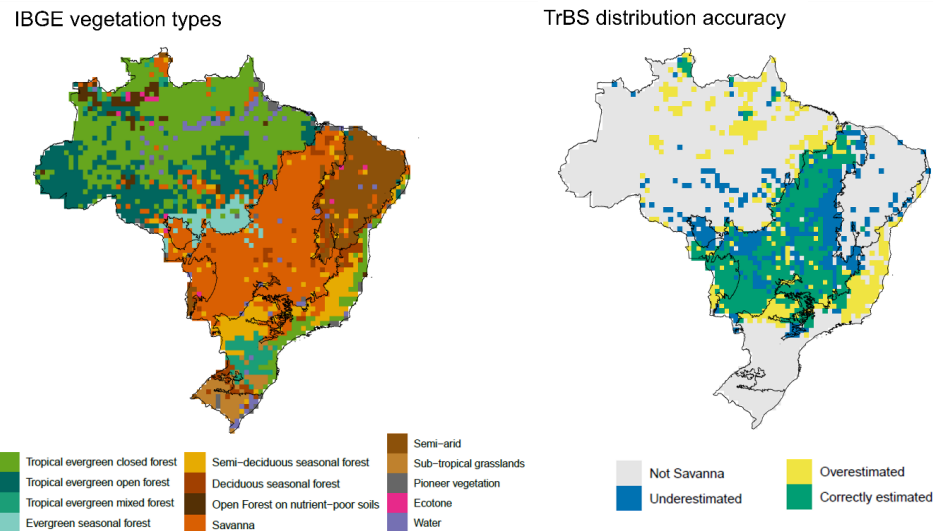
483 Fig. 4: Maps showing the Brazilian vegetation types according to IBGE (left) and TrBS

484 PFT distribution accuracy (right) in comparison with the savanna vegetation class from

485 IBGE. A threshold of 30% FPC cover was used to determine distribution accuracy.

486

487 **3.2 Above- and belowground Biomass and vegetation structure**

488 The inclusion of TrBS PFT significantly improved the simulated above- and

489 belowground biomass patterns across Brazil compared to simulations without it. By better

490 capturing the characteristic small trees with extensive belowground structures of the

491 Cerrado, TrBS PFT led to an improved representation of the 'upside-down forest' in central

492 Brazil (Fig. 5). As a reflection of the distinct allocation strategies of the Cerrado

493   vegetation, the biomass ratio (BGB:AGB) was also clearly improved in the Savanna

494   scenario (Fig. 5). Although the simulated values did not fully match those observed in the

495   QCN validation, as shown by the Spearman correlations (QCN vs. Savanna: 0.27; QCN

496   vs. No Savanna: -0.16), the introduction of TrBS resulted in a more accurate simulation of

497   carbon allocation across Brazil. Normalized Mean Error (NME) and correlation of

498   modelled ET and GPP across Brazil were in a similar range for both simulations in

499   comparison to the reference data (Fig. S9; Table S3).

500   TrBS PFT also improved the representation of tree height gradients, with tall trees,

501   above 20 m, in the Amazon transitioning to slightly shorter trees in the southern Amazon

502   and reaching approximately 7 m in the Cerrado (Fig. 5; Fig. S7). Additionally, the model

503   now captures a gradient in rooting depth (D95), with shallower roots in the Amazon,

504   deepening towards the southern Amazon and Cerrado (Fig. 5; Fig. S7). This pattern is

505   further supported by a higher D95:height ratio in the Cerrado, aligning with the

506   characterization of its vegetation as an 'upside-down forest,' where rooting depth can

507   exceed tree height.

508

509
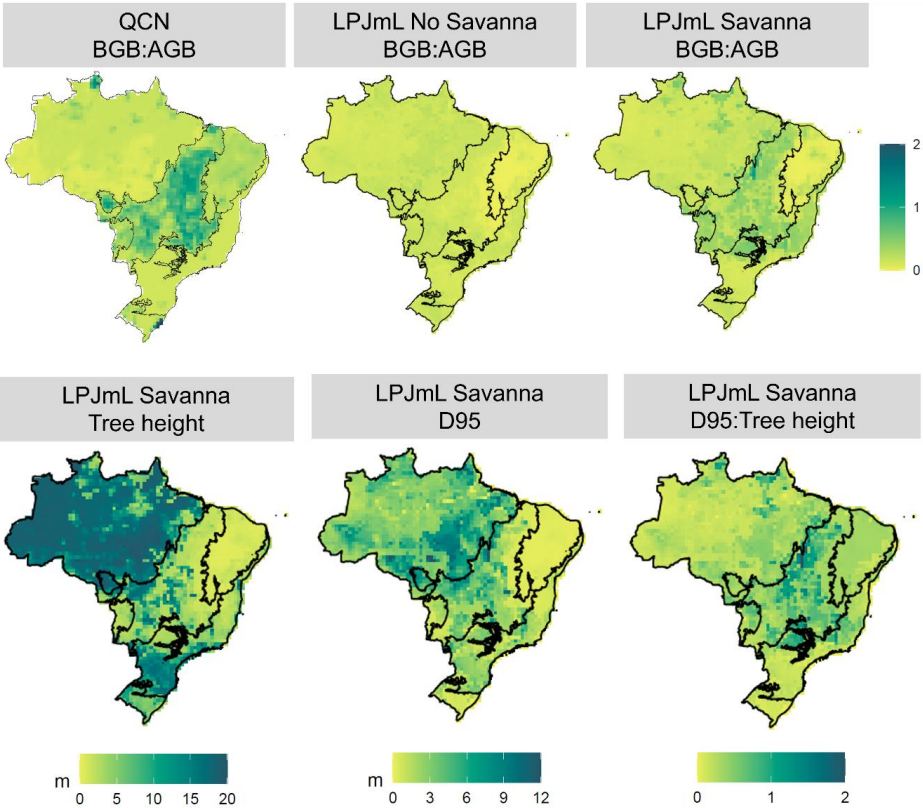
Fig. 5: FPC-weighted BGB:AGB below- and aboveground biomass ratio (BGB:AGB)

from LPJmL simulations and QCN validation product (top row), and FPC-weighted tree

height and D95, and their ratio (D95:Tree height) from LPJmL 'Savanna' simulation

(bottom row).

514

3.3 Fire dynamics

516 The introduction of TrBS PFT significantly influenced burned area patterns across

biomes. LPJmL-VR-SPITFIRE generally underestimated burned areas in the 'No

Savanna' simulation, particularly in the Cerrado and Amazon regions, while

overestimating them in the Caatinga (Table 3; Fig. 6). With the inclusion of the new TrBS

PFT, the burned area estimates in the Cerrado increased, surpassing the values recorded in

521 the MapBiomas Fogo in the central Cerrado, but still underestimating burned area in the

522 northern region (Fig. 6). In contrast, the Amazon continued to show underestimations of

523 burned areas, likely due to the general assumption of higher human-caused ignitions in

524 rural areas not capturing the real motivations to set fire. Despite these regional

525 discrepancies and given the SPITFIRE improvements applied to both model

526 configurations, the inclusion of TrBS PFT and its adjusted parameterisations led to a clear

527 improvement in the total burned area estimates for Brazil (Table 3).

528

529 Table 3: Total burned area for all Brazilian biomes simulated by LPJmL-VR-SPITFIRE

530 for 'Savanna', and 'No Savanna' scenarios, and the validation data from MapBiomas

531 Fogo. The values are in Thousand hectares (Kha).

	Savanna (Kha)	No Savanna (Kha)	MapBiomas (Kha)
Cerrado	6660.7	2597.21	7748.43
Amazon	405.67	44.48	4991.57
Atlantic Forest	89.69	5.82	130.83
Caatinga	2937.68	2818.43	345.6
Pantanal	203.84	5.33	558.55
Pampa	1.15	1.15	11.89
Brazil	**10298.73**	**5472.42**	**13786.89**

532

533

534
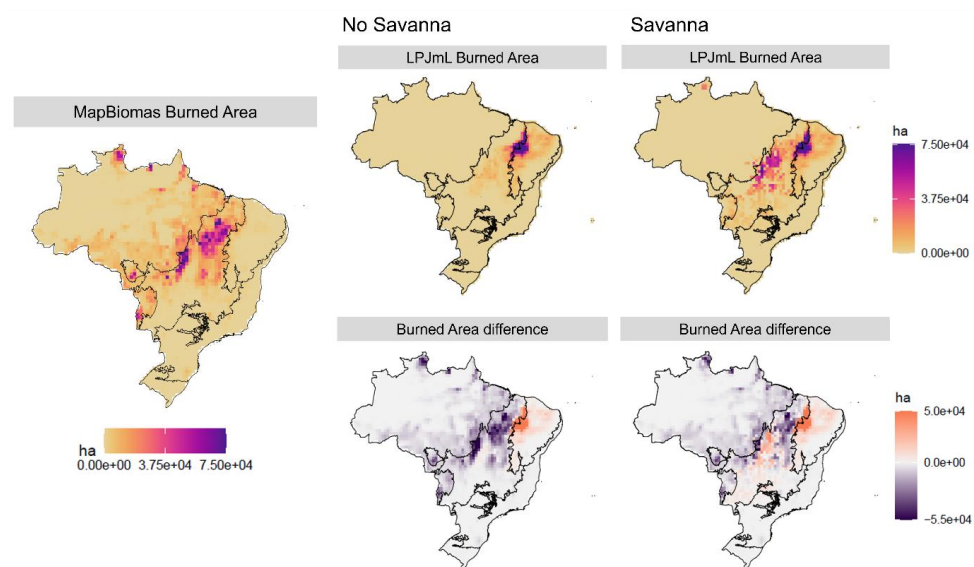
Fig. 6: LPJmL simulations of burned area in Brazil for 'No Savanna' and 'Savanna'
scenarios (top row), the validation data by MapBiomas Fogo (left), and the respective
difference between simulated results and MapBiomas Fogo validation (bottom row).

538

We could also observe an improvement in the seasonal patterns of the burned area in
the Cerrado Biome with the incorporation of TrBS PFT (Fig. 7). The Savanna scenario,
compared to the MapBiomas data, shows an NMSE of 0.39 with an R^2 of 0.45, and a
Willmott index of 0.81, indicating that the model has a good fit. The No Savanna scenario
has a slightly higher NMSE (0.83) and Willmott index (0.86), and a lower R^2 (0.40)
compared to MapBiomas, suggesting that removing TrBS reduces the overall model's
ability to represent observed seasonal fire patterns.

546
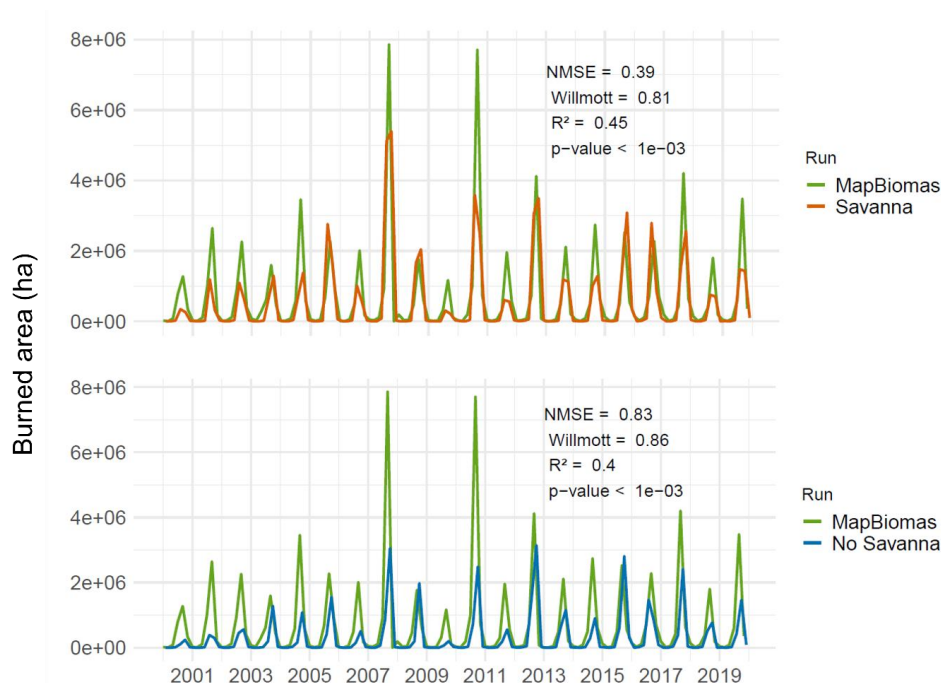
Fig. 7: Total monthly burned area, for the Cerrado Biome, from 2000 to 2019 for two LPJmL simulation scenarios: Savanna' (top) and 'No Savanna' (bottom) in comparison with the monthly burned area product from MapBiomas Fogo.

Carbon emission by fire (FireC) patterns reflect directly the burned area patterns (Fig. 8). Overall, the introduction of TrBS did not improve emission estimates in Brazil as most of the emission comes from southeastern Amazon, which has its burned area highly underestimated by our model. Fire-related emissions in the Cerrado, on the other hand, were overestimated in the Savanna scenario, especially in the central portion of the biome, which is linked to the spatial burned area patterns.
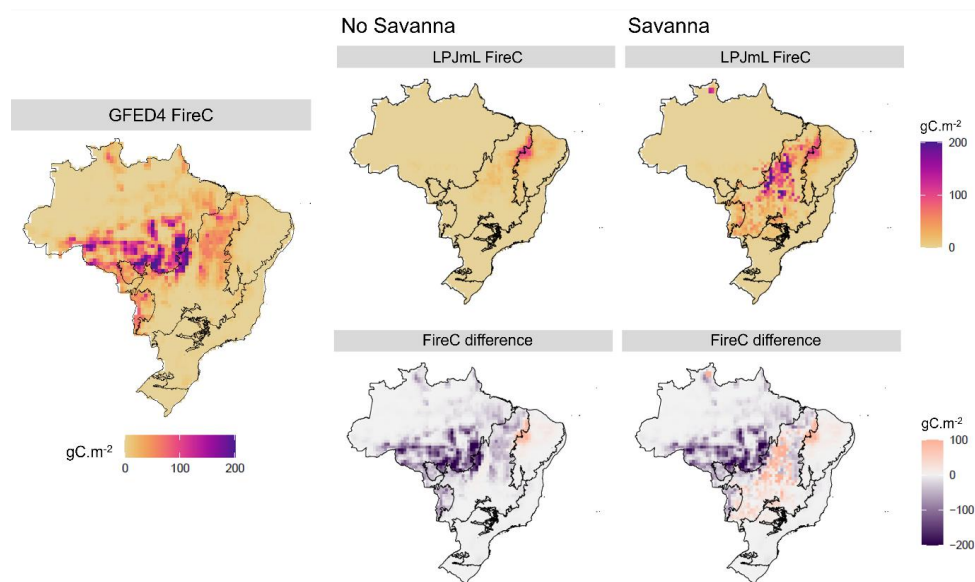
Fig. 8: LPJmL simulations of Fire carbon emission in Brazil for No Savanna and Savanna

scenarios (top row), the validation data by GFED4 (left), and the respective difference

between simulated results and GFED4 validation (bottom row).

3.4 Extrapolation to the global scale

Since the LPJmL-VR-SPITFIRE model will also be run on a global scale in future

applications, the parameterization of the new PFT was tested in a global simulation using

the same climate input data set as for the Brazilian simulations. Although TrBS PFT was

specifically adapted to the Cerrado tree data, we found high agreement in the simulated

global savanna distribution compared to a reference dataset (Hengl et al., 2018). The

results are shown in Supplementary Fig. S8.

4. Discussion

4.1 Advancing in Savanna Modeling

The introduction of a savanna-specific Plant Functional Type in the LPJmL-VR-SPITFIRE model significantly enhances the representation of vegetation and fire dynamics in Brazil. TrBS improved simulations of carbon allocation, particularly below- to aboveground biomass ratio, and better represented fire behavior, namely the spatial distribution and temporal dynamics of burned area. Key features of the Cerrado, that also apply to tropical savannas in general, are now well represented: a vegetation that is adapted to seasonal drought environments by accessing water with deep root systems and allocating more resources belowground and can cope with or even depends on regular occurring fires. This update moves the capability of LPJmL-VR-SPITFIRE beyond the previous binary classification of tropical rainforests and grasslands, allowing for a more nuanced depiction of ecological transitions, such as the Amazon-Cerrado interface. By incorporating savanna vegetation, the model facilitates more realistic investigations into the future dynamics of these biomes and allows for a more critical evaluation of restoration efforts within this specific vegetation type. A model limited to representing only 'forest' and 'grasslands' will fail to capture the significance and vulnerabilities inherent in savanna ecosystems like the Cerrado.

Other DGVMs have struggled earlier to accurately depict the savanna biome (Whitley et al., 2017; Baudena et al., 2015), as many of them oversimplify root dynamics, specific phenology and vegetation-fire feedback. In particular, the role of rooting depth, which is often constrained to shallow values in DGVMs, has a significant impact on the competition between forest, savanna vegetation and grasses, as shown by Langan et al., (2017) for South America. The introduction of root growth and rooting depth diversity in the LPJmL model (Sakschewski et al., 2021) can therefore be considered key to improving savanna

597   modeling, as it allows vegetation adaptation to water scarcity, especially when subdividing

598   the PFTs into different rooting strategies. Importantly, the competition for water between

599   savanna trees and grasses can also be better depicted when partitioning of access to water

600   resources is considered (Whitley et al., 2017; Baudena et al., 2015).

601   The SPITFIRE model provided a process-based calculation of ignition, fire spread and

602   tree fire mortality that is central to better reproduce typical Cerrado and savanna biome

603   characteristics. However, the often-extensive use of fire for land management purposes in

604   savannas (and, for example, also the edges of Amazonia) is not explicitly reflected in

605   SPITFIRE, as the model only considers a function of population density to calculate

606   ignition risks. Recent attempts to better reflect anthropogenic fire management (Perkins et

607   al., 2024) could help further improve Cerrado fire modeling. Given the increasing pressure

608   on the Cerrado and already observed shifts in fire regimes (da Silva Arruda et al., 2024),

609   this is key to enabling simulations of future trajectories in the region. While accurate fire-

610   vegetation dynamics are crucial for realistic biome distribution simulations, they are

611   insufficient if key vegetation characteristics, such as deep root water uptake, are not

612   adequately represented (D'Onofrio et al., 2020, Baudena et al., 2015).

613   We parameterized the savanna tree PFT using field and literature data specific to the

614   Brazilian Cerrado region and achieved a good fit between modelled and observed savanna

615   distribution. Other modeling studies, for example Moncrieff et al., (2016), have

616   encountered challenges to capture the Cerrado extent due to missing processes.

617   Extrapolations of model parametrization that were specifically evaluated for one savanna

618   region, here the Cerrado, often leads to inaccuracies, given the distinct climate, species

619   composition, and fire-vegetation interactions in each of the savanna-type regions (Solbrig

620   et al., 1996; Lehmann et al., 2014; Moncrieff et al., 2016). Nevertheless, to assess the

621   robustness of our parameterization, we conducted a global simulation and found that the

622   parameterization developed for the Brazilian savanna performed well in simulating global

623   tropical savanna distributions (Fig. S7). Future work could also include an assessment to

624   better capture main functional differences between each savanna-type region.

625

626   *4.2 Challenges in Representing the Cerrado Dynamics*

627   Despite these advancements, several challenges remain in capturing the complex

628   vegetation dynamics of the Cerrado. Although our simulations already produce a mix of

629   savanna trees and grasses in the northern Cerrado, one key issue is achieving a realistic

630   balance and dynamic feedback between tree and grass cover. Achieving a more realistic

631   vegetation structure is challenging with representing tree and shrub individuals as

632   generalized representatives of each PFT, even though differentiations by rooting depth

633   were incorporated in LPJmL-VR-SPITFIRE. Building on the knowledge gained in this

634   study a gap-model framework that simulates individual trees and also incorporates trait

635   diversity such as the LPJmL-FIT model (Sakschewski et al., 2015; Thonicke et al., 2020),

636   could offer a more accurate representation of tree-grass coexistence in the near future.

637   Our analysis focused on depicting the overall distribution and performance of the new

638   savanna PFT across Brazil. A detailed, site specific validation of carbon and water fluxes,

639   the seasonality of leaf cover and productivity might complement the results of this study.

640   In this context, further model refinement could be undertaken, such as implementing shade

641   intolerant PFTs in the model (Ronquim et al., 2003; Lemos-Filho et al., 2010).

642   Additionally, a notable limitation observed in our simulations is the overrepresentation of

643   C_4 grasses in the Caatinga biome, which contrasts with the known vegetation

644   characteristics of the region. The Caatinga is a semi-arid biome characterized by diverse

645   vegetation physiognomies, including succulents and small shrub vegetation, with a

646   predominance of seasonal dry tropical forests rather than extensive grasslands (de Queiroz

647 et al., 2017). In follow-up work with LPJmL-VR-SPITFIRE, it should be determined

648 which PFT combination is closest to this complex real-world vegetation. As discussed for

649 the tree-grass coexistence in the previous paragraph, Caatinga vegetation modeling would

650 benefit from an individual tree approach (as in LPJmL-FIT) rather than the average

651 individual approach of the LPJmL model. Addressing this will be important for improving

652 model realism and its applicability to drier tropical ecosystems, as well as enhancing its

653 performance in representing fire patterns in the region.

654   Fire impacts on the vegetation are a key process that maintains savannas' open-canopy

655 structure. Our parameterization of the savanna tree PFT resulted in a vegetation type that

656 is readily burning, while being well protected against lethal damage from fire. However,

657 resprouting mechanisms, which are crucial for post-fire recovery (Souchie at al. 2017) are

658 not yet implemented explicitly in the vegetation model but would improve the simulation

659 of vegetation recovery. The amount of fuel available for burning is another key area of

660 ongoing model development, as it strongly influences fire spread and intensity. In the most

661 recent SPITFIRE version that we used in this study, the live grass moisture calculation was

662 substantially improved (Oberhagemann et al., 2025), better reflecting seasonal dynamics

663 of fuel availability of grass vegetation. However, currently live woody materials are not

664 parametrized as part of the burnable matter in SPITFIRE, but this is potentially important

665 in Cerrado (Oliveira et al., 2021).

666   In Savannas, there is often extensive use of fire for land management purposes.

667 Specifically, in the Cerrado, fire in natural areas is associated with the use of fire for

668 deforestation, with fire escaping to natural areas and also with pasture management; in

669 areas of mechanized agriculture and planted forests, owners rather protect the areas against

670 fire. The underestimation in burned area observed in southeastern Amazon is also a product

671 of such land-use change practices, especially the usage of fire to manage large extension

672   of pasturelands in Amazon (MapBiomas Fogo, 2024) which could possibly escape and

673   damage adjacent tropical rainforest (Cano-Crespo et al., 2015). The SPITFIRE model does

674   not explicitly account for different fire management regimes but scales ignitions to human

675   population density. This might explain the lack of fire at the edges of Amazonia in our

676   simulations and also complicates validation of burned area and fire carbon emissions from

677   our PNV simulations. We therefore weighed both validation data and model output by the

678   human landuse fraction from MapBiomas to exclude grid cells with extensive human land

679   use from the analysis.

680   The most recent version of LPJmL incorporates the nitrogen cycle (von Bloh et al.,

681   2018), along with mechanisms of biological nitrogen fixation (BNF, Wirth et al., 2024).

682   Soils in the Cerrado are characterized by acidity, high aluminum concentrations, and

683   nutrient scarcity (Bustamante et al., 2006; 2012), requiring vegetation to develop specific

684   adaptations that confer a competitive advantage in these nutrient-poor conditions. Future

685   advancements should leverage these model enhancements to incorporate nitrogen and

686   other nutrient constraints, enhancing ecological realism to specifically address this aspect

687   to the complex ecological interactions.

688   Beyond the factors already discussed, rootable soil depth significantly influences

689   vegetation dynamics. However, determining the maximum depth roots can physically

690   penetrate is challenging, as they can grow into bedrock and access groundwater, but are

691   also limited by high soil density and low oxygen availability. In our simulations we used

692   the water table depth of Guiglemo et al., (2021) as a proxy for rootable soil depth, which

693   allows deep rooting over large parts of the Cerrado, in line with observations of deep

694   rooting vegetation. While this method provides reasonably spatial variable maximum

695   rooting depths, LPJmL-VR-SPITFIRE does not simulate an actual water table. In reality,

696   deep-rooted trees can tap groundwater, but LPJmL-VR-SPITFIRE assumes free drainage,

697   preventing this interaction. Consequently, some areas may experience artificially shallow

698   rooting depths (e.g. Amazonian floodplains) without the benefit of accessing deeper water

699   reserves, a factor that could become important, especially when running future simulations

700   with the model. Considering these aspects in future work, especially global studies, could

701   further improve the representation of belowground competition and resulting spatial

702   vegetation distribution.

703

704   **5.   Conclusion**

705   The parameterization of the new Tropical Broadleaved Savanna PFT (TrBS) in LPJmL-

706   VR-SPITFIRE significantly improves the representation of the Cerrado biome, the second-

707   largest vegetation formation in South America, in terms of belowground vs aboveground

708   competition, vegetation dynamics and fire. By inclusion of variable rooting strategies

709   along with recent process-based fire modeling, and a new drought mortality function, we

710   present a model that is suited to study complex ecological interactions of the sensitive

711   Cerrado biome that are rapidly changing under ongoing climate change. Here, we

712   combined literature and observational data to parameterize the TrBS PFT and to adjust

713   parameters of tree and root allocation functions, among others. Introducing a dedicated

714   vegetation type for tropical savannas and combining with variable rooting strategies will

715   equip DGVMs to make more precise assessments of recovery, reforestation, and

716   regeneration strategies in these unique ecosystems. By refining the modeling of savanna

717   dynamics, this study provides a valuable foundation for improving conservation strategies,

718   land-use planning, and climate mitigation efforts in fire-prone landscapes such as the

719   Cerrado. The introduction of a savanna-specific PFT with deeper rooting depth not only

720   led to a more realistic allocation of carbon belowground but also enabled the model to

721   reproduce the iconic "upside-down forest" structure of the Cerrado. This structural realism

722 also translated into better representation of vegetation distribution, fire regimes, and their

723 seasonal patterns. These results underscore the importance of incorporating trait diversity,

724 particularly rooting strategies, into DGVMs. Building on this progress, future work, such

725 as extending this savanna-specific PFT to individual-based models like LPJmL-FIT, can

726 further enhance our understanding of post-fire recovery dynamics interacting with

727 functional diversity and more clearly distinguish the intrinsic ecological behavior of

728 tropical savannas from that of tropical forests.

729

730 **6. Code and Data Availability**

731 The LPJmL-VR-SPITFIRE model is open-source and available at [*link will be added in*

732 *future*]. Field survey data used in this study are available from the corresponding author

733 upon reasonable request. All other relevant data supporting the findings of this study are

734 available from the authors or included in the supplementary materials.

735

736 **7. Competing interests**

737 One author is a member of the editorial board of journal "Biogeosciences".

738

739 **8. Author contributions**

740 *J.S.: Data curation, Formal analysis, Visualization, Writing – original draft

741 *S.B.: Methodology and Software, Formal analysis, Visualization, Writing – original

742 draft

743 W.v.B.: Methodology and Software, Writing – review and editing

744 M.Bi.: Methodology and Software, Writing – review and editing

745 B.S.: Conceptualization, Writing – review and editing

746 L.O.: Writing – review and editing

747   K.Th.: Supervision, Writing – review and editing

748   M.Bu.: Supervision, Writing – review and editing

749

750   **9. Acknowledgments**

751   The authors are grateful to PIK and the Graduate Program in Ecology from UnB for

752   providing the infrastructure and assistance without which this project wouldn't be possible.

753   To all researchers from the Ecosystems in Transition group at PIK and the Ecosystems

754   Ecology Lab at UnB that contributed with suggestions, critiques, points and ideas. Special

755   thanks to Letícia Gomes, Isabel Castro, Waira Machida, Lucas Costa and Felipe Lenti for

756   sharing their field data, essential for this work. Boris Sakschewski is part of the Planetary

757   Boundaries Science Lab.

758

759   **10. Funding Information**

760   J.S. acknowledges the funding by the National Coordination for High Level Education and

761   Training (CAPES) through the Internationalization Program (PrInt), grant number

762   88887.891863/2023-00. This work was supported by the National Institute of Science and

763   Technology for Climate Change Phase 2 under CNPq grant 465501/2014-1, FAPESP grant

764   2014/50848-9 and CAPES grant 88881.146050/2017-01. S.B. gratefully acknowledges

765   funding by the Conservation International Foundation, grant number CI-114129. This

766   project has received funding from the European Union's Horizon 2020 research and

767   innovation program under grant agreement No 101003890 (FirEUrisk). The authors

768   gratefully acknowledge the Ministry of Research, Science and Culture (MWFK) of Land

769   Brandenburg for supporting this project by providing resources on the high-performance

770   computer system at the Potsdam Institute for Climate Impact Research.

771

772 **11. References**

773 Balsamo, G., Albergel, C., Beljaars, A., Boussetta, S., Brun, E., Cloke, H., Dee, D., Dutra,
774   E., Muñoz-Sabater, J., Pappenberger, F., de Rosnay, P., Stockdale, T., and Vitart, F.:
775   ERA-Interim/Land: A global land surface reanalysis data set, Hydrol. Earth. Syst. Sc.,
776   19, 389–407, https://doi.org/10.5194/hess-19-389-2015, 2015.

777 Baudena, M., Dekker, S. C., Van Bodegom, P. M., Cuesta, B., Higgins, S. I., Lehsten, V.,
778   Reick, C. H., Rietkerk, M., Scheiter, S., Yin, Z., Zavala, M. A., and Brovkin, V.: Forests,
779   savannas, and grasslands: Bridging the knowledge gap between ecology and Dynamic
780   Global Vegetation Models, Biogeosciences, 12, 1833–1848, https://doi.org/10.5194/bg-
781   12-1833-2015, 2015.

782 Bowman, D. M. J. S., Balch, J. K., Artaxo, P., Bond, W. J., Carlson, J. M., Cochrane, M.
783   A., D'Antonio, C. M., DeFries, R. S., Doyle, J. C., Harrison, S. P., Johnston, F. H.,
784   Keeley, J. E., Krawchuk, M. A., Kull, C. A., Marston, J. B., Moritz, M. A., Prentice, I.
785   C., Roos, C. I., Scott, A. C., … Pyne, S. J: Fire in the Earth System, Science, 324, 481–
786   484, https://doi.org/10.1126/science.1163886, 2009.

787 Bustamante, M. M. C., Nardoto, G. B., Pinto, A. S., Resende, J. C. F., Takahashi, F. S. C.,
788   and Vieira, L. C. G.: Potential impacts of climate change on biogeochemical functioning
789   of Cerrado ecosystems. Braz. J. Biol., 72, 655–671, https://doi.org/10.1590/S1519-
790   69842012000400005, 2012.

791 Bustamante, M. M. C., Silva, J. S., Scariot, A., Sampaio, A. B., Mascia, D. L., Garcia, E.,
792   Sano, E., Fernandes, G. W., Durigan, G., Roitman, I., Figueiredo, I., Rodrigues, R. R.,
793   Pillar, V. D., de Oliveira, A. O., Malhado, A. C., Alencar, A., Vendramini, A., Padovezi,
794   A., Carrascosa, H., … Nobre, C.: Ecological restoration as a strategy for mitigating and
795   adapting to climate change: Lessons and challenges from Brazil. Mitig. Adapt. Stra.t Gl.,
796   24, 1249–1270, https://doi.org/10.1007/s11027-018-9837-5, 2019.

797 Bustamante, M., Medina, E., Asner, G., Nardoto, G., and Garcia-Montiel, D.: Nitrogen
798   cycling in tropical and temperate savannas, Biogeochemistry, 79, 209–237,
799   https://doi.org/10.1007/s10533-006-9006-x, 2006.

800   Cano-Crespo, A., Oliveira, P. J. C., Boit, A., Cardoso, M., and Thonicke, K.: Forest edge
801   burning in the Brazilian Amazon promoted by escaping fires from managed pastures, J.
802   Geophys. Res-Biogeo., 120, 2095-2107, https://doi.org/10.1002/2015JG002914, 2015.

803   Carvalhais, N., Forkel, M., Khomik, M., Bellarby, J., Jung, M., Migliavacca, M., Mu, M.,
804   Saatchi, S., Santoro, M., Thurner, M., Weber, U., Ahrens, B., Beer, C., Cescatti, A.,
805   Randerson, J. T., and Reichstein, M.: Global covariation of carbon turnover times with
806   climate in terrestrial ecosystems, Nature, 51, 213–217,
807   https://doi.org/10.1038/nature13731, 2014.

808   Christian, H. J., Blakeslee, R. J., Boccippio, D. J., Boeck, W. L., Buechler, D. E., Driscoll,
809   K. T., Goodman, S. J., Hall, J. M., Koshak, W. J., Mach, D. M., and Stewart, M. F.:
810   Global frequency and distribution of lightning as observed from space by the Optical
811   Transient Detector, J. Geophys.. Res-Atmos, 108, ACL 4-1-ACL 4-15,
812   https://doi.org/10.1029/2002JD002347, 2003.

813   Costa, L.: Nutrient enrichment changes water transport structures of savanna woody plants,
814   figshare, https://doi.org/10.6084/m9.figshare.13252052.v1, 2020.

815   Cramer, W., Bondeau, A., Woodward, F. I., Prentice, I. C., Betts, R. A., Brovkin, V., Cox,
816   P. M., Fisher, V., Foley, J. A., Friend, A. D., Kucharik, C., Lomas, M. R., Ramankutty,
817   N., Sitch, S., Smith, B., White, A., and Young-Molling, C.: Global response of terrestrial
818   ecosystem structure and function to CO_2 and climate change: Results from six dynamic
819   global vegetation models, Glob. Change Biol., 7, 357–373,
820   https://doi.org/10.1046/j.1365-2486.2001.00383.x, 2001.

821   de Camargo, M. G. G., de Carvalho, G. H., Alberton, B. D. C., Reys, P., and Morellato, L.
822   P. C.: Leafing patterns and leaf exchange strategies of a cerrado woody community.
823   Biotropica, 50, 442–454. https://doi.org/10.1111/btp.12552, 2018.

824   D'Onofrio, D., Baudena, M., Lasslop, G., Nieradzik, L. P., Wårlind, D., and von
825   Hardenberg, J.: Linking vegetation-climate-fire relationships in Sub-Saharan Africa to
826   key ecological processes in two dynamic global vegetation models, Fr. Environ. Sci, 8,
827   https://doi.org/10.3389/fenvs.2020.00136, 2020.

828   de Queiroz, L.P., Cardoso, D., Fernandes, M.F., Moro, M.F: Diversity and Evolution of
829   Flowering Plants of the Caatinga Domain., In: Silva, J.M.C., Leal, I.R., Tabarelli, M.
830   (eds) Caatinga. Springer-Cham, https://doi.org/10.1007/978-3-319-68339-3_2, 2017.

831   Drüke, M., Forkel, M., von Bloh, W., Sakschewski, B., Cardoso, M., Bustamante, M.,
832   Kurths, J., and Thonicke, K.: Improving the LPJmL4-SPITFIRE vegetation–fire model
833   for South America using satellite data,   Geosci. Model Dev., 12, 5029–5054,
834   https://doi.org/10.5194/gmd-12-5029-2019, 2019.

835   Feron, S., Cordero, R. R., Damiani, A., MacDonell, S., Pizarro, J., Goubanova, K.,
836   Valenzuela, R., Wang, C., Rester, L., and Beaulieu, A.: South America is becoming
837   warmer,   drier,   and   more   flammable.   Commun.   Earth   Environ.,   5,   501,
838   https://doi.org/10.1038/s43247-024-01654-7, 2024.

839   Forkel, M., Carvalhais, N., Schaphoff, S., V. Bloh, W., Migliavacca, M., Thurner, M., and
840   Thonicke, K.: Identifying environmental controls on vegetation greenness phenology
841   through   model–data   integration.   Biogeosciences,   11,   7025–7050.
842   https://doi.org/10.5194/bg-11-7025-2014, 2014.

843   Gomes, L., Miranda, H. S., and Bustamante, M. M. C.: How can we advance the knowledge
844   on the behavior and effects of fire in the Cerrado biome? Forest Ecol. Manag., 417, 281–
845   290. https://doi.org/10.1016/j.foreco.2018.02.032, 2018.

846   Gomes, L., Miranda, H. S., Soares-Filho, B., Rodrigues, L., Oliveira, U., and Bustamante,
847   M. M. C.: Responses of plant biomass in the Brazilian savanna to frequent fires, Front.
848   Forest Glob. Change, 3, 507710. https://doi.org/10.3389/ffgc.2020.507710, 2020a.

849   Gomes, L., Miranda, H. S., Silvério, D. V., and Bustamante, M. M. C.: Effects and
850   behaviour of experimental fires in grasslands, savannas, and forests of the Brazilian
851   Cerrado,   Forest   Ecol.   Manag.   458,   117804.
852   https://doi.org/10.1016/j.foreco.2019.117804, 2020b.

853   Gomes, L., Schüler, J., Silva, C., Alencar, A., Zimbres, B., Arruda, V., Silva, W. V. da,
854   Souza, E., Shimbo, J., Marimon, B. S., Lenza, E., Fagg, C. W., Miranda, S., Morandi, P.
855   S., Marimon-Junior, B. H., and Bustamante, M.: Impacts of fire frequency on net CO_2

856   emissions in the Cerrado savanna vegetation, Fire, 7, 208,

857   https://doi.org/10.3390/fire7080280, 2024.

858   Grimm, A. M., Vera, C. S., and Mechoso, C. R.: The South American monsoon system,

859   In: The Global Monsoon System: Research and Forecast, WMO/TD 1266, TMRP

860   Rep. 70, 219–238, Available at https://core.ac.uk/download/pdf/36730348.pdf, 2005.

861   Guglielmo, M., Tang, F. H. M., Pasut, C., and Maggi, F.: SOIL-WATERGRIDS,

862   mapping dynamic changes in soil moisture and depth of water table from 1970 to

863   2014, Scient. Data, 8, 263. https://doi.org/10.1038/s41597-021-01032-4, 2021.

864   Hengl, T., Walsh, M. G., Sanderman, J., Wheeler, I., Harrison, S. P., and Prentice, I. C.:

865   Global mapping of potential natural vegetation: An assessment of machine learning

866   algorithms for estimating land potential, PeerJ, 6, e5457,

867   https://doi.org/10.7717/peerj.5457, 2018.

868   Hoffmann, W. A., Adasme, R., Haridasan, M., T. De Carvalho, M., Geiger, E. L., Pereira,

869   M. A. B., Gotsch, S. G., and Franco, A. C.: Tree topkill, not mortality, governs the

870   dynamics of savanna–forest boundaries under frequent fire in central Brazil, Ecology,

871   90, 1326–1337, https://doi.org/10.1890/08-0741.1, 2009.

872   Hoffmann, W. A., da Silva, E. R., Machado, G. C., Bucci, S. J., Scholz, F. G., Goldstein,

873   G., and Meinzer, F. C.: Seasonal leaf dynamics across a tree density gradient in a

874   Brazilian savanna, Oecologia, 145, 306–315, https://doi.org/10.1007/s00442-005-0129-

875   x, 2005.

876   Hoffmann, W. A., Orthen, B., and Franco, A. C.: Constraints to seedling success of savanna

877   and forest trees across the savanna-forest boundary, Oecologia, 140, 252–260,

878   https://doi.org/10.1007/s00442-004-1595-2, 2004.

879   Hofmann, G., Cardoso, M., Alves, R., Weber, E., Barbosa, A., De Toledo, P., Pontual, F.,

880   Salles, L., Hasenack, H., Passos Cordeiro, J. L., Aquino, F., and Oliveira, L.: The

881   Brazilian Cerrado is becoming hotter and drier, Glob. Change Biol., 27,

882   https://doi.org/10.1111/gcb.15712, 2021.

883 IBGE: Brazilian Vegetation, Available at
884 https://www.ibge.gov.br/en/geosciences/maps/state-maps/19470-brazilian-
885 vegetation.html?=andt=downloads, 2017.

886 IBGE: Biomas e Sistema Costeiro-Marinho do Brasil—PGI, Available at
887 https://www.ibge.gov.br/apps/biomas/#/home, 2024.

888 Jackson, R. B., Canadell, J., Ehleringer, J. R., Mooney, H. A., Sala, O. E., and Schulze, E.
889 D.: A global analysis of root distributions for terrestrial biomes, Oecologia, 108, 389–
890 411. https://doi.org/10.1007/BF00333714, 1996.

891 Klein Goldewijk, K., Beusen, A., Drecht, G., and Vos, M.: The HYDE 3.1 spatially explicit
892 database of human-induced global land-use change over the past 12,000 years, Global
893 Ecol Biogeogr., 20, 73–86, https://doi.org/10.1111/j.1466-8238.2010.00587.x, 2011.

894 Langan, L., Higgins, S. I., and Scheiter, S.: Climate-biomes, pedo-biomes or pyro-biomes:
895 which world view explains the tropical forest–savanna boundary in South America? J.
896 Biogeogr., 44, 2319–2330, https://doi.org/10.1111/jbi.13018, 2017.

897 Lehmann, C. E. R., Anderson, T. M., Sankaran, M., Higgins, S. I., Archibald, S., Hoffmann,
898 W. A., Hanan, N. P., Williams, R. J., Fensham, R. J., Felfili, J., Hutley, L. B., Ratnam,
899 J., San Jose, J., Montes, R., Franklin, D., Russell-Smith, J., Ryan, C. M., Durigan, G.,
900 Hiernaux, P., … Bond, W. J.: Savanna vegetation-fire-climate relationships differ among
901 continents. Science, 343, 548–552, https://doi.org/10.1126/science.1247355, 2014.

902 Machida, W. S., Gomes, L., Moser, P., Castro, I. B., Miranda, S. C., da Silva-Júnior, M.
903 C., and Bustamante, M. M. C.: Long term post-fire recovery of woody plants in
904 savannas of central Brazil, Forest Ecol. Manag., 493, 119255.
905 https://doi.org/10.1016/j.foreco.2021.119255, 2021.

906 Malhi, Y., Aragão, L. E. O. C., Galbraith, D., Huntingford, C., Fisher, R., Zelazowski, P.,
907 Sitch, S., McSweeney, C., and Meir, P.:Exploring the likelihood and mechanism of a
908 climate-change-induced dieback of the Amazon rainforest, P. Natl. A. Sci., 106, 20610–
909 20615, https://doi.org/10.1073/pnas.0804619106, 2009.

910 MapBiomas 9.0: MapBiomas Uso e Cobertura 9.0, Available at
911 https://brasil.mapbiomas.org/colecoes-mapbiomas/, 2024.

912   MapBiomas   Fogo: MapBiomas   Fogo   3.0,   Available   at
913   https://mapbiomasfogocol3v1.netlify.app/index.html, 2024.

914   Martens, C., Hickler, T., Davis-Reddy, C., Engelbrecht, F., Higgins, S. I., Von Maltitz, G.
915   P., Midgley, G. F., Pfeiffer, M., and Scheiter, S.: Large uncertainties in future biome
916   changes in Africa call for flexible climate adaptation strategies, Glob. Change Biol., 27,
917   340–358 https://doi.org/10.1111/gcb.15390, 2021.

918   MCTI: Quarto inventário nacional de emissões e remoções antrópicas de gases de efeito
919   estufa setor uso da terra, mudança do uso da terra e florestas, Available at:
920   https://repositorio.mcti.gov.br/handle/mctic/4782, 2020.

921   MCTI: First biennial transparency report of Brazil to the United Nations Framework
922   Convention   on   Climate   Change,   Available   at: https://www.gov.br/mcti/pt-
923   br/acompanhe-o-mcti/sirene/publicacoes/relatorios-bienais-de-transparencia-btrs, 2024.

924   Moncrieff, G. R., Scheiter, S., Langan, L., Trabucco, A., and Higgins, S. I.: The future
925   distribution of the savannah biome: model-based and biogeographic contingency, Philos.
926   T. R. Soc. B., 371, 20150311, https://doi.org/10.1098/rstb.2015.0311, 2016.

927   Myers, N., Mittermeier, R. A., Mittermeier, C. G., da Fonseca, G. A. B., and Kent, J.:
928   Biodiversity   hotspots   for   conservation   priorities,   Nature,   403,   853–858.
929   https://doi.org/10.1038/35002501, 2000.

930   Oberhagemann, L., Billing, M., Von Bloh, W., Drüke, M., Forrest, M., Bowring, S. P. K.,
931   Hetzer, J., Ribalaygua Batalla, J., and Thonicke, K.: Sources of uncertainty in the global
932   fire model SPITFIRE: development of LPJmL-SPITFIRE1.9 and directions for future
933   improvements, Geosci. Model Dev., 18, 2021-2025, https://doi.org/10.5194/gmd-18-
934   2021-2025, 2025.

935   Oliveira, R. S., Bezerra, L., Davidson, E. A., Pinto, F., Klink, C. A., Nepstad, D. C., and
936   Moreira, A.: Deep root function in soil water dynamics in cerrado savannas of central
937   Brazil. Funct. Ecol., 19, 574–581, https://doi.org/10.1111/j.1365-2435.2005.01003.x,
938   2005.

939   Oliveira, U., Soares-Filho, B., de Souza Costa, W. L., Gomes, L., Bustamante, M., and
940   Miranda, H.: Modeling fuel loads dynamics and fire spread probability in the Brazilian

941   Cerrado,   Forest   Ecol.   Manag.,   482,   118889,
942   https://doi.org/10.1016/j.foreco.2020.118889, 2021.

943   Oliver, T. H., Heard, M. S., Isaac, N. J. B., Roy, D. B., Procter, D., Eigenbrod, F.,
944   Freckleton, R., Hector, A., Orme, C. D. L., Petchey, O. L., Proença, V., Raffaelli, D.,
945   Suttle, K. B., Mace, G. M., Martín-López, B., Woodcock, B. A., and Bullock, J. M:
946   Biodiversity and resilience of ecosystem functions. Trends Ecol. Evol., 30, 673–684,
947   https://doi.org/10.1016/j.tree.2015.08.009, 2015.

948   Peel, M. C., Finlayson, B. L., and McMahon, T. A.: Updated world map of the Köppen-
949   Geiger   climate   classification,   Hydrol.   Earth   Syst.   Sc.,   11,   1633–1644,
950   https://doi.org/10.5194/hess-11-1633-2007, 2007.

951   Perkins, O., Kasoar, M., Voulgarakis, A., Smith, C., Mistry, J., and Millington, J. D. A.
952   (2024). A global behavioural model of human fire use and management: WHAM! v1.0,
953   Geosci. Model Dev., 17, 3993–4016, https://doi.org/10.5194/gmd-17-3993-2024, 2024.

954   Pivello, V. R.: The Use of fire in the Cerrado and amazonian rainforests of Brazil: past and
955   present. Fire Ecol., 7, 24-39. https://doi.org/10.4996/fireecology.0701024, 2011.

956   Ratnam, J., Bond, W. J., Fensham, R. J., Hoffmann, W. A., Archibald, S., Lehmann, C. E.
957   R., Anderson, M. T., Higgins, S. I., and Sankaran, M.: When is a 'forest' a savanna, and
958   why does it matter? Global Ecol. Biogeogr., 20, 653–660. https://doi.org/10.1111/j.1466-
959   8238.2010.00634.x, 2011.

960   Ribeiro, J., and Walter, B.: As principais fitofisionomias do bioma Cerrado In: Sano, S.M.,
961   Almeida, S.P. and Ribeiro, J.F. (Eds.), Cerrado Ecologia e Flora, p. 152–212., 2008.

962   Rodrigues, A. A., Macedo, M. N., Silvério, D. V., Maracahipes, L., Coe, M. T., Brando, P.
963   M., Shimbo, J. Z., Rajão, R., Soares-Filho, B., and Bustamante, M. M. C.: Cerrado
964   deforestation threatens regional climate and water availability for agriculture and
965   ecosystems, Glob. Change Biol., 28, 6807–6822, https://doi.org/10.1111/gcb.16386,
966   2022.

967   Ronquim, C. C., Prado, C. H. B. de A., and de Paula, N. F.: Growth and photosynthetic
968   capacity in two woody species of cerrado vegetation under different radiation

availability, Braz. Arch. Biol. Techn., 46, 243–252, https://doi.org/10.1590/S1516-89132003000200016, 2003.

Saboya, P., and Borghetti, F.: Germination, initial growth, and biomass allocation in three native Cerrado species, Braz. J. Bot., 35, 129–135, https://doi.org/10.1590/S0100-84042012000200002, 2012.

Sakschewski, B., Von Bloh, W., Boit, A., Rammig, A., Kattge, J., Poorter, L., Peñuelas, J., and Thonicke, K.: Leaf and stem economics spectra drive diversity of functional plant traits in a dynamic global vegetation model, Glob. Change Biol., 21, 2711–2725, https://doi.org/10.1111/gcb.12870, 2015.

Sakschewski, B., von Bloh, W., Drüke, M., Sörensson, A. A., Ruscica, R., Langerwisch, F., Billing, M., Bereswill, S., Hirota, M., Oliveira, R. S., Heinke, J., and Thonicke, K.: Variable tree rooting strategies are key for modelling the distribution, productivity and evapotranspiration of tropical evergreen forests. Biogeosciences, 18, 4091–4116, https://doi.org/10.5194/bg-18-4091-2021, 2021.

Salazar, A., Katzfey, J., Thatcher, M., Syktus, J., Wong, K., and McAlpine, C.: Deforestation changes land–atmosphere interactions across South American biomes, Global Planet. Change, 139, 97–108, https://doi.org/10.1016/j.gloplacha.2016.01.004, 2016.

Sano, E. E., Rodrigues, A. A., Martins, E. S., Bettiol, G. M., Bustamante, M. M. C., Bezerra, A. S., Couto, A. F., Vasconcelos, V., Schüler, J., and Bolfe, E. L.: Cerrado ecoregions: A spatial framework to assess and prioritize Brazilian savanna environmental diversity for conservation, J. Environ. Manage., 232, 818–828, https://doi.org/10.1016/j.jenvman.2018.11.108, 2019.

Schaphoff, S., Von Bloh, W., Rammig, A., Thonicke, K., Biemans, H., Forkel, M., Gerten, D., Heinke, J., Jägermeyr, J., Knauer, J., Langerwisch, F., Lucht, W., Müller, C., Rolinski, S., and Waha, K.: LPJmL4 – a dynamic global vegetation model with managed land – Part 1: Model description. Geosci. Model Dev., 11, 1343–1375, https://doi.org/10.5194/gmd-11-1343-2018, 2018.

997   Scholz, F. G., Bucci, S. J., Goldstein, G., Meinzer, F. C., Franco, A. C., and Salazar, A.:
998   Plant- and stand-level variation in biophysical and physiological traits along tree density
999   gradients in the Cerrado, Braz. J. Plant Physiol., 20, 217–232,
1000   https://doi.org/10.1590/S1677-04202008000300006, 2008.

1001 Schüler, J.: Áreas prioritárias para a restauração no Cerrado: aumentando os benefícios e
1002   reduzindo os conflitos, Masters dissertation, Universidade de Brasília, 105 p. Available
1003   at http://repositorio.unb.br/handle/10482/39518, 2020.

1004 Schüler, J., and Bustamante, M. M. C.: Spatial planning for restoration in Cerrado:
1005   Balancing the trade-offs between conservation and agriculture, J. Appl. Ecol., 59, 2616–
1006   2626, https://doi.org/10.1111/1365-2664.14262, 2022.

1007 Schumacher, V., Setzer, A., Saba, M. M. F., Naccarato, K. P., Mattos, E., and Justino, F.:
1008   Characteristics of lightning-caused wildfires in central Brazil in relation to cloud-ground
1009   and dry lightning. Agr. Forest Meteorol., 312, 108723,
1010   https://doi.org/10.1016/j.agrformet.2021.108723, 2022.

1011 Shinozaki, K., Yoda, K., Hozumi, K., and Kira, T.: A quantitative analysis of plant form-
1012   the Pipe Model Theory: II. Further evidence of the theory and its application in forest
1013   ecology. Jpn. J. Ecol., 14, 133–139. https://doi.org/10.18960/seitai.14.4_133, 1964.

1014 Simon, M. F., and Pennington, T.: Evidence for adaptation to fire regimes in the tropical
1015   savannas of the Brazilian Cerrado, Int. J. Plant Sci., 173, 711–723,
1016   https://doi.org/10.1086/665973, 2012.

1017 Solbrig, O. T., Medina, E., and Silva, J. F.: Biodiversity and savanna ecosystem processes:
1018   A global perspective (Vol. 121). Springer, 1996.

1019 Souchie, F. F., Pinto, J. R. R., Lenza, E., Gomes, L., Maracahipes-Santos, L., and Silvério,
1020   D. V.: Post-fire resprouting strategies of woody vegetation in the Brazilian savanna, Acta
1021   Bot. Bras., 31, 260–266, https://doi.org/10.1590/0102-33062016abb0376, 2017.

1022 Souza, C. R. D., Coelho De Souza, F., Françoso, R. D., Maia, V. A., Pinto, J. R. R., Higuchi,
1023   P., Silva, A. C., Prado Júnior, J. A. D., Farrapo, C. L., Lenza, E., Mews, H., Rocha, H.
1024   L. L., Mota, S. L., Rodrigues, A. L. C., Silva-Sene, A. M. D., Moura, D. M., Araújo, F.
1025   D. C., Oliveira, F. D., Gianasi, F. M., … Santos, R. M. D.: Functional and structural

1026 attributes of Brazilian tropical and subtropical forests and savannas, Forest Ecol. Manag.,
1027 558, 121811, https://doi.org/10.1016/j.foreco.2024.121811, 2024.

1028 Strassburg, B. B. N., Brooks, T., Feltran-Barbieri, R., Iribarrem, A., Crouzeilles, R., Loyola,
1029 R., Latawiec, A. E., Oliveira Filho, F. J. B., Scaramuzza, C. A. de M., Scarano, F. R.,
1030 Soares-Filho, B., and Balmford, A.: Moment of truth for the Cerrado hotspot, Nat. Ecol.
1031 Evol., 1, 1–3, https://doi.org/10.1038/s41559-017-0099, 2017.

1032 Swann, A. L. S., Longo, M., Knox, R. G., Lee, E., and Moorcroft, P. R.: Future deforestation
1033 in the Amazon and consequences for South American climate, Agr. Forest Meteorol.,
1034 214–215, 12–24, https://doi.org/10.1016/j.agrformet.2015.07.006, 2015.

1035 Syktus, J. I., and McAlpine, C. A.: More than carbon sequestration: Biophysical climate
1036 benefits of restored savanna woodlands, Sci. Rep-UK, 6, 29194,
1037 https://doi.org/10.1038/srep29194, 2016.

1038 Terra, M. C. N. S., Nunes, M. H., Souza, C. R., Ferreira, G. W. D., Prado-Junior, J. A. do,
1039 Rezende, V. L., Maciel, R., Mantovani, V., Rodrigues, A., Morais, V. A., Scolforo, J. R.
1040 S., and Mello, J. M.: The inverted forest: Aboveground and notably large belowground
1041 carbon stocks and their drivers in Brazilian savannas, Sci. Total Environ., 867, 161320,
1042 https://doi.org/10.1016/j.scitotenv.2022.161320, 2023.

1043 Terra, M. D. C. N. S., Santos, R. M. D., Prado Júnior, J. A. D., De Mello, J. M., Scolforo,
1044 J. R. S., Fontes, M. A. L., Schiavini, I., Dos Reis, A. A., Bueno, I. T., Magnago, L. F. S.,
1045 and Ter Steege, H.: Water availability drives gradients of tree diversity, structure and
1046 functional traits in the Atlantic–Cerrado–Caatinga transition, Brazil, J. Plant Ecol., 11,
1047 803–814, https://doi.org/10.1093/jpe/rty017, 2018.

1048 Thonicke, K., Billing, M., von Bloh, W., Sakschewski, B., Niinemets, Ü., Peñuelas, J.,
1049 Cornelissen, J. H. C., Onoda, Y., van Bodegom, P., Schaepman, M. E., Schneider, F. D.,
1050 and Walz, A.: Simulating functional diversity of European natural forests along climatic
1051 gradients, J Biogeogr., 47, 1069–1085, https://doi.org/10.1111/jbi.13809, 2020.

1052 Thonicke, K., Spessa, A., Prentice, I. C., Harrison, S. P., Dong, L., and Carmona-Moreno,
1053 C.: The influence of vegetation, fire spread and fire behavior on biomass burning and

1054   trace gas emissions: Results from a process-based model, Biogeosciences, 7, 1991–2011,
1055   https://doi.org/10.5194/bg-7-1991-2010, 2010.

1056   Tumber-Dávila, S. J., Schenk, H. J., Du, E., and Jackson, R. B.: Plant sizes and shapes above
1057   and belowground and their interactions with climate, New Phytol., 235, 1032–1056,
1058   https://doi.org/10.1111/nph.18031, 2022.

1059   van der Werf, G. R., Randerson, J. T., Giglio, L., van Leeuwen, T. T., Chen, Y., Rogers, B.
1060   M., Mu, M., van Marle, M. J. E., Morton, D. C., Collatz, G. J., Yokelson, R. J., and
1061   Kasibhatla, P. S.: Global fire emissions estimates during 1997–2016, Earth Syst. Sci.
1062   Data, 9, 697–720, https://doi.org/10.5194/essd-9-697-2017, 2017.

1063   Von Bloh, W., Schaphoff, S., Müller, C., Rolinski, S., Waha, K., and Zaehle, S.:
1064   Implementing the nitrogen cycle into the dynamic global vegetation, hydrology, and crop
1065   growth model LPJmL (version 5.0), Geosci. Model Dev., 11, 2789–2812,
1066   https://doi.org/10.5194/gmd-11-2789-2018, 2018.

1067   Whitley, R., Beringer, J., Hutley, L. B., Abramowitz, G., De Kauwe, M. G., Evans, B.,
1068   Haverd, V., Li, L., Moore, C., Ryu, Y., Scheiter, S., Schymanski, S. J., Smith, B., Wang,
1069   Y.-P., Williams, M., and Yu, Q.: Challenges and opportunities in land surface modelling
1070   of savanna ecosystems, Biogeosciences, 14, 4711–4732, https://doi.org/10.5194/bg-14-
1071   4711-2017, 2017.

1072   Wirth, S. B., Braun, J., Heinke, J., Ostberg, S., Rolinski, S., Schaphoff, S., Stenzel, F., von
1073   Bloh, W., Taube, F., and Müller, C.: Biological nitrogen fixation of natural and
1074   agricultural vegetation simulated with LPJmL 5.7.9, Geosci. Model Dev., 17, 7889–
1075   7914, https://doi.org/10.5194/gmd-17-7889-2024, 2024.

1076   Wullschleger, S. D., Epstein, H. E., Box, E. O., Euskirchen, E. S., Goswami, S., Iversen, C.
1077   M., Kattge, J., Norby, R. J., van Bodegom, P. M., and Xu, X.: Plant functional types in
1078   Earth system models: Past experiences and future directions for application of dynamic
1079   vegetation models in high-latitude ecosystems, Ann. Bot-London, 114, 1–16.
1080   https://doi.org/10.1093/aob/mcu077, 2014.

1081   Zemp, D. C., Schleussner, C.-F., Barbosa, H. M. J., Hirota, M., Montade, V., Sampaio, G.,
1082   Staal, A., Wang-Erlandsson, L., and Rammig, A.: Self-amplified Amazon forest loss due

1083   to vegetation-atmosphere feedbacks, Nature Commun., 8, 14681,

1084   https://doi.org/10.1038/ncomms14681, 2017.